Radboud Repository

Radboud University Nijmegen

PDF hosted at the Radboud Repository of the Radboud University Nijmegen

The following full text is a publisher's version.

For additional information about this publication click this link.
http://hdl.handle.net/2066/35057

Accurate quantum calculations of the reaction rates for H/D+CH$_4$

Rob van Harrevelt,[a] Gunnar Nyman,[b] and Uwe Manthe
Theoretische Chemie, Universität Bielefeld, Universitätsstrasse 25, D-33615 Bielefeld, Germany

In previous work [T. Wu, H. J. Werner, and U. Manthe, Science **306**, 2227 (2004)], accurate quantum reaction rate calculations of the rate constant for the H+CH$_4$→CH$_3$+H$_2$ reaction have been presented. Both the electronic structure calculations and the nuclear dynamics calculations are converged with respect to the basis sets employed. In this paper, the authors apply the same methodology to an isotopic variant of this reaction: D+CH$_4$→CH$_3$+HD. Accurate rate constants are presented for temperatures between 250 and 400 K. For temperatures between 400 and 800 K, they use a harmonic extrapolation to obtain approximate rate constants for H/D+CH$_4$. The calculations suggest that the experimentally reported rate constants for D+CH$_4$ are about a factor of 10–20 too high. For H+CH$_4$, more accurate experiments are available and agreement is much better: the difference is less than a factor of 2.6. The kinetic isotope effect for the H/D+CH$_4$ reactions is studied and compared with experiment and transition state theory (TST) calculations. Harmonic TST was found to provide a good description of the kinetic isotope effect. © *2007 American Institute of Physics*. [DOI: 10.1063/1.2464102]

I. INTRODUCTION

The reaction H+CH$_4$→CH$_3$+H$_2$ is of fundamental interest as an elementary hydrocarbon-radical reaction. The reaction is also relevant in combustion and atmospheric chemistry. It has been the subject of many theoretical studies: reduced dimensionality quantum calculations[1–11] and quantum transition state theory based approaches[12–18] have been published by various groups. Even accurate full-dimensional quantum dynamics calculations for thermal rate constants and cumulative reaction probabilities have been presented.[19–21] In a recent study,[22,23] high-level electronic structure calculations, sophisticated interpolation schemes for the potential energy surface, and full-dimensional quantum dynamics simulations have been combined to obtain an accurate rate constant from first principles. All sources of errors have been carefully studied: the convergence with the basis set in the electronic structure and quantum dynamics calculations and the accuracy of the interpolation scheme. Only inaccuracies resulting from the coupled cluster [CCSD(T)] approach and the *J*-shifting approximation[24] could not be estimated quantitatively. If the CCSD(T) method and the *J*-shifting approximations are reasonable, then the accuracy of the *ab initio* approach can compete with, or is even better than, available experiments. The estimated numerical uncertainty in the computed rate constant is about 30%.

In previous work[22,23] the absolute value of the thermal rate constant was studied. Here, we will also examine the kinetic isotope effect (KIE) in the *X*+CH$_4$→CH$_3$+H*X* (*X*=H,D) reaction. Kurylo *et al.*[25] found experimentally that D reacts faster with methane than H. These results are quan-

titatively reproduced by theoretical studies of Pu and Truhlar,[15] who used quantum transition state theory approaches and a semiempirical potential energy surface. Since it is now possible to calculate accurate rate constants from first principles, we can predict kinetic isotope effects with high accuracy. These results are presumably more accurate than the experimental ones.

The main goal of the present study is to calculate accurate rate constants for D+CH$_4$ in the temperature range of 250–400 K. In combination with previous results for H +CH$_4$,[22,23] we can then obtain the kinetic isotope effect. A second goal of this paper is to extend rate constant calculations for H/D+CH$_4$ to higher temperatures. Accurate, fully converged quantum calculations are only possible for temperatures up to about 400–500 K. At higher temperatures, the number of vibrationally excited states of the activated complex that participates in the reaction is so large that some approximation is required. In this paper, we use a harmonic progression scheme[26] to estimate the rate constant for temperatures up to 800 K. The accuracy of this scheme is investigated in detail.

The article is organized as follows. Section II discusses the theoretical approach followed in this work. It is divided into two parts. Section II A discusses accurate reaction rate calculations. We show how a harmonic extrapolation can be used to enhance convergence of the rate constant.[26] Section II B presents a harmonic progression based approach to obtain approximate rate constants. Section III gives the numerical details and Sec. IV discusses the results. Section IV A presents accurate results for the temperature range of 250–500 K and Sec. IV B presents approximate rate constants for temperatures up to 800 K. The paper concludes with a summary and some final remarks.

[a]Present address: Radboud Universiteit Nijmegen, Nijmegen, the Netherlands.
[b]Also at Göteborgs Universitet, Göteborg, Sweden.

126, 084303-1

II. THEORY

A. Accurate reaction rate calculations

The present work employs the same theoretical and computational scheme as described in detail in Ref. 22. In this scheme, the flux-correlation formalism[27–29] is used to calculate the rate constant directly, without solving the full scattering problem. A short summary of the followed approach is given below; for further details, we refer to Ref. 22. Assuming that the J-shifting[24] approximation is valid, the rate constant k is calculated from

$$k = \frac{Q^{\ddagger}_{\text{rot}}}{2\pi\hbar Q_r} \int dE N(E) \exp(- E/k_B T), \tag{1}$$

where $Q^{\ddagger}_{\text{rot}}$ is the rotational partition function at the transition state geometry, Q_r the reactant partition function, E the total energy, and $N(E)$ the cumulative reaction probability for total angular momentum $J=0$. $N(E)$ is the quantity which is obtained from accurate quantum dynamics calculations.

The cumulative reaction probability obtained from the quantum simulations can be given as a sum of several terms $N_i(E)$: $N(E) = \Sigma_i N_i(E)$.[30] The $N_i(E)$'s correspond to different pairs of eigenstates of the thermal flux operator. Each contribution $N_i(E)$ can be considered as the contribution of the ith vibrational state of the activated complex to $N(E)$. For high temperatures, the number of states required to converge the thermal rate constant increases dramatically. To enhance the convergence with respect to the number of contributions explicitly considered, a harmonic extrapolation can be employed.[26] Assume that $N_i(E)$ is calculated for $i=0, n$. The best estimate of the rate constant based on the data for the $n+1$ lowest vibrational states of the activated complex reads as follows:[26]

$$k_n(T) = \frac{Q^{\ddagger}_{\text{rot}}}{2\pi\hbar Q_r} \frac{\sum\limits_{i=0}^{\infty} \exp(- (E_i - E_0)/k_B T)}{\sum\limits_{i=0}^{n} \exp(- (E_i - E_0)/k_B T)}$$

$$\times \int dE \left\{ \sum_{i=0}^{n} N_i(E) \right\} \exp(- E/k_B T), \tag{2}$$

where E_i is the energy of the ith vibrational state of the activated complex in harmonic approximation ($i=0$ corresponds to the ground state of the activated complex). The harmonic frequencies can be obtained from normal mode analysis at the transition state geometry. It is easy to see that $k_n(T)$ converges to the exact $k(T)$:

$$\lim_{n\to\infty} k_n(T) = k(T). \tag{3}$$

B. Approximate rate constants based on the harmonic progression

When only the ground state contribution $N_0(E)$ is explicitly included in the rate constant calculation, then Eq. (2) reduces to

$$k_0(T) = \frac{Q^{\ddagger}_{\text{rot}}}{2\pi\hbar Q_r} \sum_{i=0}^{\infty} \exp(- (E_i - E_0)/k_B T)$$

$$\times \int dE N_0(E) \exp(- E/k_B T). \tag{4}$$

Since the term $\Sigma_{i=0}^{\infty} \exp(-(E_i-E_0)/k_B T)$ is the harmonic approximation of the vibrational partition function of the transition state, $Q^{\ddagger}_{\text{vib,harm}}$, we can write

$$k_0(T) = \frac{Q^{\ddagger}_{\text{rot}} Q^{\ddagger}_{\text{vib,harm}}}{2\pi\hbar Q_r} \int dE N_0(E) \exp(- E/k_B T). \tag{5}$$

Equation (5) is identical to Eq. (1) when the $N_i(E)$'s obey

$$N_i(E) = N_0(E - (E_i - E_0)). \tag{6}$$

This expression is the vibrational analog to the J-shifting approximation[24] for rotational motion. Here, the vibration orthogonal to the reaction path is treated similarly as the overall rotation of the complex in the J-shifting approximation. In this paper, we will show that Eq. (5) can be a very useful approximation to the rate constant.

The approximate expression for the rate constant, Eq. (5), also makes the relation with harmonic transition state theory (TST) more transparent. Harmonic TST assumes that $N_0(E) = \Theta(E - E_b)$, where Θ is the Heaviside step function and E_b is the vibrationally adiabatic barrier height in the harmonic approximation. Then, since $\int dE N_0(E) \exp(-E/k_B T) = k_B T \exp(-E_b/k_B T)$,

$$k^{\text{TST}}(T) = k_B T \frac{Q^{\ddagger}_{\text{rot}} Q^{\ddagger}_{\text{vib,harm}}}{2\pi\hbar Q_r} \exp(- E_0/k_B T). \tag{7}$$

It should be noted that any theory based on the harmonic approximation for the transition state should also use the harmonic approximation to describe the vibrational excitation energies in the reactant partition function Q_r.[31]

III. NUMERICAL DETAILS

The 12-dimensional wave packet is propagated using the multiconfiguration time dependent Hartree (MCTDH) approach.[32–35] The coordinates used in the MCTDH wave packet propagation are obtained from a linear transformation of transition state normal mode coordinates. The harmonic frequencies for the transition state normal modes on the present potential energy surface are presented in Table I. The reason why a transformation of normal modes is advantageous in the MCTDH calculations is discussed in Refs. 19 and 20. Mode 1 (the mode with the imaginary frequency) is mixed with one other mode:

$$\begin{pmatrix} Q'_1 \\ Q'_k \end{pmatrix} = \begin{pmatrix} \cos\gamma & -\sin\gamma \\ \sin\gamma & \cos\gamma \end{pmatrix} \begin{pmatrix} Q_1 \\ Q_k \end{pmatrix}. \tag{8}$$

The two modes Q_1 and Q_k largely correspond to the motion of the H/D atoms located on the C_{3v} symmetry axis. Mode k is 9 and 7 for H+CH_4 and D+CH_4, respectively. The other transition state normal mode coordinates are not transformed. In this work, we employ $\gamma = 20°$ for both systems. The dividing surface can now be defined as $Q'_1 = 0$, and the

TABLE I. Harmonic frequencies at the transition state geometry (in cm^{-1}), including the imaginary frequency (mode Q_1). Note that some modes are doubly degenerate as they correspond to the E irreducible representation of the C_{3v} point group.

	H−CH$_4$		D−CH$_4$
Modes	Frequency	Modes	Frequency
Q_1	1414i	Q_1	1414i
Q_2, Q_3	534	Q_2, Q_3	484
Q_4	1073	Q_4	1006
Q_5, Q_6	1124	Q_5, Q_6	1104
Q_7, Q_8	1442	Q_7	1393
Q_9	1795	Q_8, Q_9	1442
Q_{10}	3076	Q_{10}	3076
Q_{11}, Q_{12}	3232	Q_{11}, Q_{12}	3232

transformed coordinates Q_i' are employed in the dynamical calculations.

The parameters used to represent the wave function, the numbers of single particle functions and the grid sizes, are based on extensive convergence tests. The procedure has been described in detail in Refs. 20–22. Table II gives the parameters for the converged D+CH$_4$ calculations. Parameters for H+CH$_4$ have the same values as in previous work.[22,23]

An important parameter in the quantum dynamics simulations is the reference temperature T_{ref}.[36,37] The results are formally independent of T_{ref}. However, this parameter determines the energy range where the computed $N(E)$ is reliable. This range corresponds to those energies where $N(E)$ $\exp(-E/k_B T_{ref})$ makes a significant contribution to the integral in Eq. (1). To obtain the results presented below, different reference temperatures have been used to study different temperature ranges.

IV. RESULTS AND DISCUSSION

A. Accurate rate constants for D+CH$_4$ and the kinetic isotope effect

Using a reference temperature of $T_{ref}=300$ K, we obtained accurate rate constants for the temperature range of 250–400 K. Rate constants are presented in Table III and plotted in Fig. 1. Figure 1 also shows the harmonic TST result and the experimental data of Kurylo et al.[25] The dif-

TABLE II. Parameters for the MCTDH representation of the wave function for D+CH$_4$.

Coordinate	Number of single-particle functions	Grid size	Grid type	Grid range for FFT (a.u.)
Q_1'	6	48	FFT	−92−96
Q_2/Q_3	4	32	Hermite DVR	
Q_4	3	48	FFT	−60−132
Q_5/Q_6	3	18	Hermite DVR	
Q_7'	5	48	FFT	−115−80
Q_8/Q_9	2	8	Hermite DVR	
Q_{10}	2	8	Hermite DVR	
Q_{11}/Q_{12}	2	8	Hermite DVR	

TABLE III. Rate constants (in cm^3/s) for H+CH$_4\rightarrow$CH$_2$+H$_2$/D+CH$_4$ $\rightarrow$CH$_3$+HD: results of accurate quantum calculations (Refs. 22, 23, and 38) (H+CH$_4$) and the present work (D+CH$_4$).

T (K)	H+CH$_4$	D+CH$_4$
250	3.6×10^{-21}	1.2×10^{-20}
300	7.8×10^{-20}	2.2×10^{-19}
350	9.5×10^{-19}	2.3×10^{-18}
400	7.3×10^{-18}	1.6×10^{-17}

ference between TST and accurate quantum results clearly demonstrates the role of tunneling. The experimental results are higher than the present result, probably due to side reactions such as D+CH$_3\rightarrow$CH$_2$D+H in the experiment.[25]

In the present calculation, six states of the activated complex, i.e., the ground state and the first five vibrationally excited states, have been considered explicitly. We used the harmonic extrapolation, Eq. (2) to estimate the contributions of the higher excited states. The estimated contributions of higher excited states are rather small: in total 2% at 300 K and 10% at 400 K. By studying the dependence of the rate constant on the number of vibrationally excited states (n) included explicitly, we can gain insight into the accuracy of the harmonic extrapolation scheme. The differences between the rate constants obtained with $n=0$, 1, 2, 3, 4, and 5 are negligible when the harmonic extrapolation is used. As an example, Fig. 1 shows the results for both $n=0$ and $n=5$. This suggests that the harmonic extrapolation yields a reliable estimate of the effect of the excited states not included explicitly. In this case, it would have been sufficient to calculate $N_0(E)$, i.e., the contribution of the ground state of the activated complex. The contributions of all other states could be evaluated using the harmonic extrapolation [Eq. (5)]. Table IV gives the values of the rate constant obtained using
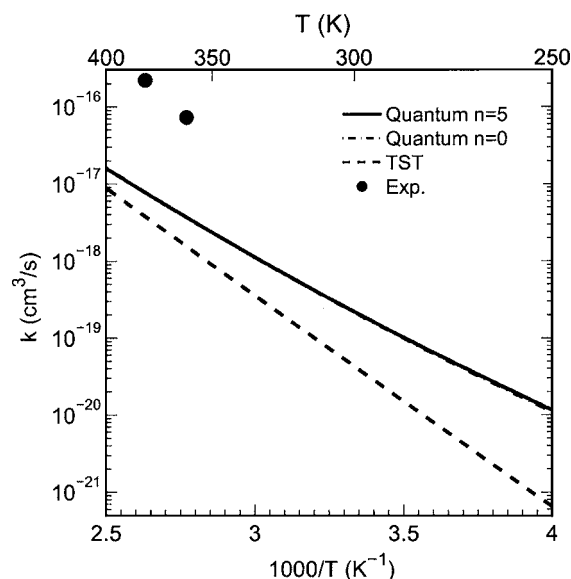

FIG. 1. Rate constants for the D+CH$_4\rightarrow$CH$_3$+HD reaction. n is the number of vibrationally excited states of the activated complex included explicitly in the accurate quantum calculations [see Eq. (2)]. Experimental rate constants are taken from Ref. 25.

TABLE IV. Approximate rate constants (in cm^3/s) for H+CH$_4$→CH$_3$+H$_2$ and D+CH$_4$→CH$_3$+HD calculated using Eq. (5). Two reference temperatures (T_{ref}) have been used to cover different temperature ranges. The H+CH$_4$, T_{ref}=300 K results are based on calculations presented in Refs. 22 and 23.

	H+CH$_4$		D+CH$_4$	
T (K)	T_{ref}=300 K	T_{ref}=500 K	T_{ref}=300 K	T_{ref}=500 K
250	3.4×10^{-21}		1.1×10^{-20}	
300	7.8×10^{-20}		2.2×10^{-19}	
350	9.8×10^{-19}	1.1×10^{-18}	2.3×10^{-18}	2.4×10^{-18}
400	7.6×10^{-18}	8.5×10^{-18}	1.6×10^{-17}	1.6×10^{-17}
450		4.5×10^{-17}		8.0×10^{-17}
500		1.8×10^{-16}		3.0×10^{-16}
600		1.6×10^{-15}		2.5×10^{-15}
700		8.3×10^{-15}		1.2×10^{-14}
800		3.0×10^{-14}		4.1×10^{-14}

FIG. 3. The kinetic isotope effect (k_{H+CH_4}/k_{D+CH_4}). Solid line: the KIE based on accurate quantum results for H+CH$_4$ (Refs. 22 and 23) and D+CH$_4$ (this work). Dashed line: harmonic TST result. Dashed-dotted line: experiment (Ref. 25).

this approach at selected temperatures: the harmonically approximated rates differ by less than 10% from the accurate ones.

The success of the harmonic extrapolation scheme can also be seen in the cumulative reaction probabilities (see Fig. 2). For a detailed investigation of the energy shifting scheme, Eq. (6), Fig. 2(b) shows $N_0(E)$ and the shifted contributions $N_1(E+(E_1-E_0))$ and $N_2(E+(E_2-E_0))$, where E_i-E_0 is the energy difference in harmonic approximation. To a good approximation, the $N_1(E)$ and $N_2(E)$ obey $N_i(E+(E_i-E_0))=N_0(E)$, which is equivalent to Eq. (6).

Using the rate constant for the H+CH$_4$→CH$_3$+H$_2$ reaction obtained in previous work[22,23] the KIE for H/D+CH$_4$ can be calculated. The individual rate constants for both reactions are given in Table III.[38] The KIE (the ratio of the H+CH$_4$ to the D+CH$_4$ rate) is presented in Fig. 3. The rate constants for H+CH$_4$ and D+CH$_4$ are obtained using the same potential energy surface and computational approach. Errors due to inaccuracies of the potential energy surface, in particular, the barrier height, should largely cancel in the calculated KIE. However, the dynamical calculations are converged with respect to basis set parameters independently. Consequently, inaccuracies of the dynamical calculations, which are expected to be in the 10%–20% range, might add up in the computed KIE. The KIE is therefore expected to be accurate to within about 20%. The numerical
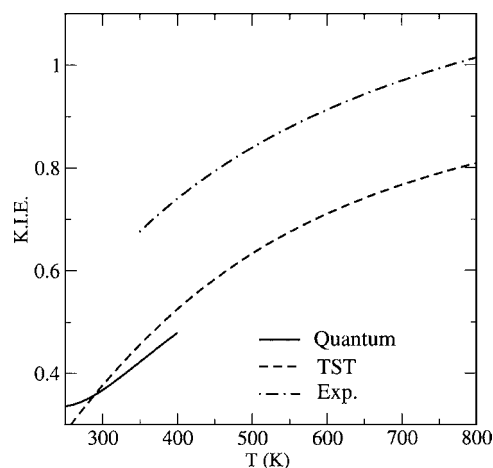
error could be temperature dependent. Considering the numerical uncertainty, the difference between the TST and quantum results is not significant.

Thus, the kinetic isotope effect is adequately described by harmonic TST, even in the temperature range where tunneling is important. This was also found in the quantum transition state theory study of Pu and Truhlar.[15] Apparently, the tunneling enhancement $\kappa=k/k_{TST}$ is almost the same for H+CH$_4$ and D+CH$_4$. This should not be surprising. In both reactions, a hydrogen atom is transferred. The imaginary frequency modes are almost identical for H+CH$_4$ and D+CH$_4$ (see Table I). The main reason for the higher rate constant for D+CH$_4$ is the lower zero-point vibrational energy at the transition state, which is 9296 and 8992 cm^{-1} for H+CH$_4$ and D+CH$_4$, respectively.

Figure 3 includes the KIE obtained from the analysis of the experimental data of Refs. 25 and 39. The analysis is based on fits of the experimental rate constants for H+CH$_4$ and D+CH$_4$ to the Arrhenius expression $k(T)=A\exp(-E_a/k_BT)$. For the D+CH$_4$ reaction, the constant A has been scaled in order to correct for the effect of side reactions. The correction factor is based on simple collision theory[25] and should therefore be considered as a crude estimate. However, the temperature dependence of the experi-
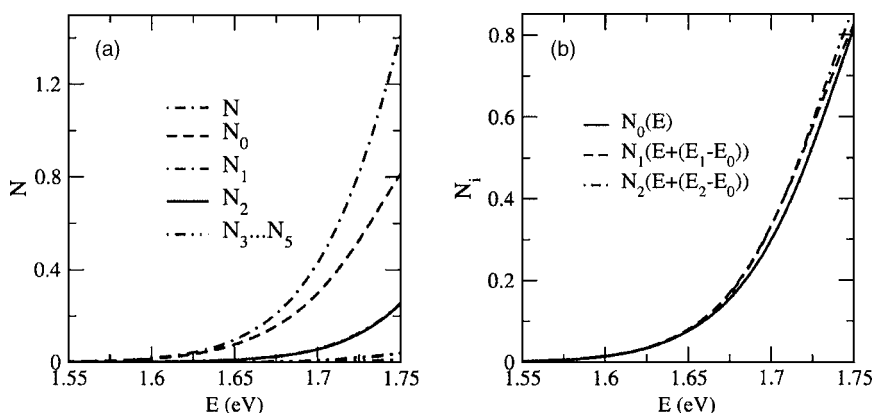

FIG. 2. Cumulative reaction probabilities for D+CH$_4$ as functions of the total energy. Panel (a): $N(E)$ and several contributions $N_i(E)$. Panel (b): The ground state contribution $N_0(E)$ and the shifted contributions $N_1(E+(E_1-E_0))$ and $N_2(E+(E_2-E_0))$.
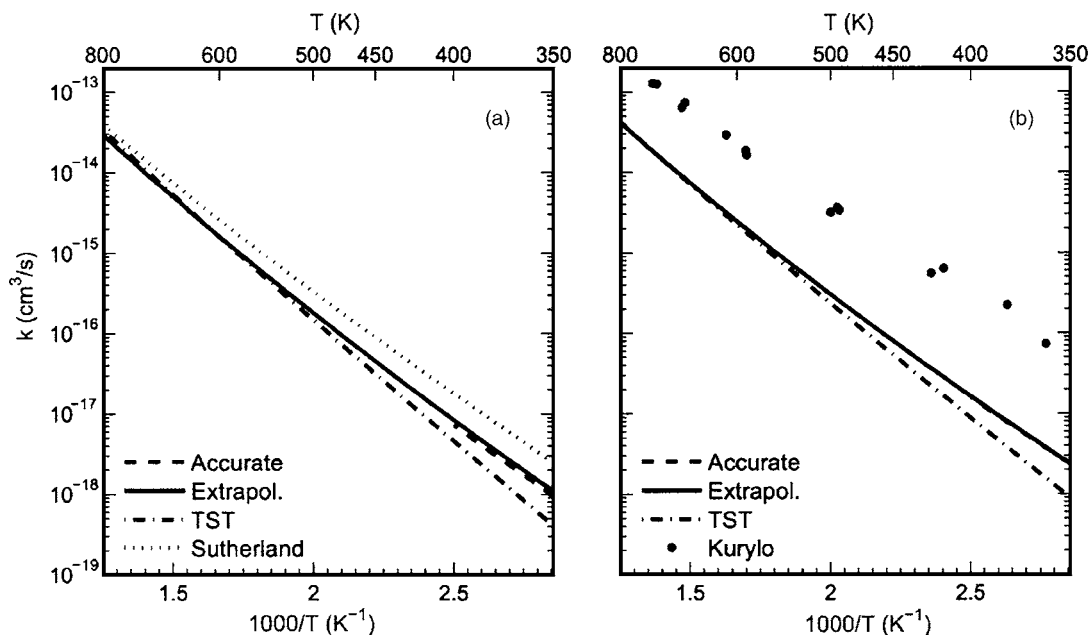
FIG. 4. Rate constants for the H+CH$_4$→CH$_3$+H$_2$ reaction [panel (a)] and D+CH$_4$→CH$_3$+HD [panel (b)] reactions: accurate quantum results ($250 \leqslant T \leqslant 400$ K), results of the harmonic extrapolation based on $N_0(E)$ ($350 \leqslant T \leqslant 800$ K), harmonic TST results, and experiment (Refs. 25 and 40).

mental KIE is probably reasonably accurate. A similar temperature dependence of the experimental and TST results can clearly been seen in Fig. 3.

B. H/D+CH$_4$ rate constants at high temperatures

To calculate the rate constants at high temperatures, $350 \leqslant T \leqslant 800$ K, we use a higher reference temperature: $T_{\mathrm{ref}}=500$ K. We further employ a harmonic progression to calculate the rate constant from the ground state contribution $N_0(E)$ to the cumulative reaction probability. In the previous section, we have shown that the harmonic extrapolation based on the ground state contribution $N_0(E)$ gives an accurate rate constant for $250 \leqslant T \leqslant 400$ K. One can reasonably expect that this approach yields a reliable estimate also at higher temperatures. The results are presented in Table IV and Fig. 4. The results obtained with the two reference temperatures differ by less than 12%, in the overlapping temperature range (350–400 K), which is consistent with the estimated numerical uncertainty, 20%, in the calculations.

Figure 4 also presents experimental rate constants. Sutherland *et al.*[40] have recently reviewed different rate constant measurements for H+CH$_4$. Based on a reanalysis of old results and new high-temperature results, they obtain an analytical expression for the rate constant that fits the available experimental results for temperatures between 350 and 1950 K. Their result is somewhat higher than the present theoretical result. However, with increasing temperature, the relative difference between theory and experiment diminishes. The ratio between the experimental and the calculated rate constants varies from 2.6 at 350 K to 1.3 at 800 K. The estimated uncertainty in the calculated result is about 30%. In contrast, experimental results at higher temperatures are likely more accurate than those at lower temperatures, where the rate constant is very low. It therefore seems reasonable to assume that at low temperatures the present theoretical re-

sults are more reliable than the available experimental data. More accurate experiments at low temperatures are required to be able to draw final conclusions.

For D+CH$_4$, the experimental rate constant is about a factor of 10–20 higher than the theoretical results, even at high temperatures. The experiments for D+CH$_4$ are more difficult than for H+CH$_4$ due to side reactions such as D+CH$_3$→CH$_2$D,[25] which might explain the large difference. Thus, additional experimental work is clearly desirable.

V. CONCLUSION

In this paper, we present calculations of the rate constant for the D+CH$_4$→CH$_3$+HD reaction. For temperatures below 400 K, we have shown that a harmonic progression of the cumulative reaction probabilities yields a reliable estimate of the rate constant. We have therefore also used this method to calculate the rate constants for temperatures up to 800 K. Using harmonic extrapolation, we have also extended previous calculations for H+CH$_4$→CH$_3$+H$_2$ (Refs. 22 and 23) to higher temperatures.

The same theoretical and computational scheme as used in Refs. 22 and 23 has been employed to calculate the cumulative reaction probabilities. It combines accurate quantum dynamics simulations with high-quality electronic structure calculations. As discussed in Ref. 22, we expect that the theoretical rate constants are accurate within about 30%. We therefore attribute the deviation of the experimental and theoretical rate constants to inaccuracies in the experiment. We hope that the present work and the work in Refs. 22 and 23 will challenge experimentalists to measure accurate rate constants for H/D+CH$_4$, in particular, at low temperatures (around 300 K), where tunneling significantly enhances the rate constant.

This paper has also examined the secondary isotope effect in the H+CH$_4$ reaction. As expected, the isotope effect

is adequately described with transition state theory, even at low temperatures were tunneling is important. Since the transferred atom is a H atom in both $H+CH_4$ and $D+CH_4$ reactions, the tunneling enhancement is almost the same.

[1] T. Takayanagi, J. Chem. Phys. **104**, 2237 (1996).
[2] H.-G. Yu and G. Nyman, J. Chem. Phys. **111**, 3508 (1999).
[3] M. Wang, Y. Li, J. Zhang, and D. Zhang, J. Chem. Phys. **113**, 1802 (2000).
[4] D. Wang and J. M. Bowman, J. Chem. Phys. **115**, 2055 (2001).
[5] H.-G. Yu, Chem. Phys. Lett. **332**, 538 (2000).
[6] J. Palma, J. Echave, and D. C. Clary, J. Phys. Chem. A **106**, 8256 (2002).
[7] M. Wang and J. Zhang, J. Chem. Phys. **117**, 3081 (2002).
[8] M. Wang and J. Zhang, J. Chem. Phys. **116**, 6497 (2002).
[9] M. Yang, D. H. Zhang, and S.-Y. Lee, J. Chem. Phys. **117**, 9539 (2002).
[10] D. Wang, J. Chem. Phys. **117**, 9806 (2002).
[11] D. Wang, J. Chem. Phys. **118**, 1184 (2003).
[12] J. Pu, J. C. Corchado, and D. G. Truhlar, J. Chem. Phys. **115**, 6266 (2001).
[13] J. Pu and D. G. Truhlar, J. Chem. Phys. **117**, 1479 (2002).
[14] J. Pu and D. G. Truhlar, J. Chem. Phys. **114**, 1468 (2001).
[15] J. Pu and D. G. Truhlar, J. Chem. Phys. **117**, 10675 (2002).
[16] J. Espinosa-Garcia, J. Chem. Phys. **116**, 10664 (2002).
[17] B. Kerkeni and D. C. Clary, J. Chem. Phys. **120**, 2308 (2004).
[18] Y. Zhao, T. Yamamoto, and W. H. Miller, J. Chem. Phys. **120**, 3100 (2004).
[19] F. Huarte-Larranaga and U. Manthe, J. Chem. Phys. **113**, 5115 (2000).
[20] F. Huarte-Larranaga and U. Manthe, J. Phys. Chem. A **105**, 2522 (2001).
[21] F. Huarte-Larranaga and U. Manthe, J. Chem. Phys. **116**, 2863 (2002).
[22] T. Wu, H. J. Werner, and U. Manthe, J. Chem. Phys. **124**, 164307 (2006).
[23] T. Wu, H. J. Werner, and U. Manthe, Science **306**, 2227 (2004).
[24] J. M. Bowman, J. Chem. Phys. **95**, 4960 (1991).
[25] M. J. Kurylo, G. A. Hollinden, and R. B. Timmons, J. Chem. Phys. **52**, 1773 (1970).
[26] F. Huarte-Larranaga and U. Manthe, J. Chem. Phys. **117**, 4635 (2002).
[27] T. Yamamoto, J. Chem. Phys. **33**, 281 (1960).
[28] W. H. Miller, J. Chem. Phys. **61**, 1823 (1974).
[29] W. H. Miller, S. D. Schwartz, and J. W. Tromp, J. Chem. Phys. **79**, 4889 (1983).
[30] U. Manthe and F. Matzkies, Chem. Phys. Lett. **282**, 442 (1998).
[31] J. M. Bowman, D. Wang, X. Huang, F. Huarte-Larranaga, and U. Manthe, J. Chem. Phys. **114**, 9683 (2001).
[32] H.-D. Meyer, U. Manthe, and L. S. Cederbaum, Chem. Phys. Lett. **165**, 73 (1990).
[33] U. Manthe, H.-D. Meyer, and L. S. Cederbaum, J. Chem. Phys. **97**, 3199 (1992).
[34] M. H. Beck, A. Jäckle, G. A. Worth, and H.-D. Meyer, Phys. Rep. **324**, 1 (2000).
[35] H.-D. Meyer and G. A. Worth, Theor. Chem. Acc. **109**, 251 (2003).
[36] U. Manthe, J. Chem. Phys. **102**, 9205 (1995).
[37] U. Manthe, J. Theor. Comput. Chem. **1**, 153 (2002).
[38] Minor errors found in the data analysis have been corrected.
[39] M. J. Kurylo and R. B. Timmons, J. Chem. Phys. **50**, 5076 (1969).
[40] J. W. Sutherland, M.-C. Su, and J. V. Michael, Int. J. Chem. Kinet. **33**, 669 (2001).